ICCFD13-2026-210

Global Stability Analysis of Compressible Flows via Continuous Local Ensemble Trained Linear Model

Ryo Takemori*, Takayuki Nagata* and Taku Nonomura*
Corresponding author: takemori.ryo.x5@s.mail.nagoya-u.ac.jp
* Department of Aerospace Engineering, Graduate School of Engineering, Nagoya University, Furo-cho, Chikusa-ku, Nagoya, Aichi 464-8603, Japan.

Abstract: While adjoint-based methods are indispensable for sensitivity analysis in modern computational fluid dynamics (CFD), their widespread application is often restricted by prohibitive implementation efforts and intrusive modifications to existing solvers. To address these challenges, this study introduces a non-intrusive, data-driven approach termed the continuous local ensemble trained linear model (CLETLM). By evaluating the residual responses to localized state perturbations within a standard forward solver, CLETLM identifies the sparse discrete Jacobian matrix. Utilizing the spatial locality inherent in numerical stencils, the framework explicitly constructs the linear operator without complex internal code alterations. As a result, the adjoint operator is easily obtained via straightforward matrix transposition, bypassing the need for dedicated adjoint codes. The proposed framework is validated through global stability and adjoint analyses of a two-dimensional compressible flow around a circular cylinder, covering Reynolds numbers from 47 to 100 and freestream Mach numbers between 0.1 and 0.3. Comparisons with existing literature show excellent agreement in both the extracted unstable eigenvalues and the spatial structures of the direct and adjoint modes. These results confirm that CLETLM accurately captures the discrete Jacobian matrix and adjoint characteristics, relying solely on forward simulation data.

Keywords: Compressible Flow, Global Stability Analysis, Adjoint Mode, Data-driven, CLETLM.

1. Introduction

In recent years, computational fluid dynamics (CFD) has evolved beyond a simple flow prediction tool into an advanced framework for discovering optimal geometries and control strategies across various industrial applications. In such optimization processes, it is crucial to efficiently calculate the gradient information—the response of objective functions to changes in design variables. The adjoint method, which provides gradient information independently of the number of design variables in massive-degree-of-freedom systems, is a particularly powerful approach. It has become an indispensable foundation for advanced analyses, including aerodynamic shape optimization [1], variational data assimilation [2], resolvent analysis [3], and balanced proper orthogonal decomposition (BPOD) [4].

However, severe implementation costs and memory constraints present significant barriers to the practical application of adjoint methods. While the discrete adjoint method [5], which explicitly retains the matrix, is relatively straightforward to implement, it demands immense memory resources for large-scale systems. Conversely, continuous adjoint methods [5] and matrix-free approaches [6] mitigate memory issues but require tremendous effort to derive adjoint equations and implement dedicated codes, forcing highly intrusive modifications to existing solvers. In addition to these implementation hurdles, compressible flows utilizing shock-capturing schemes introduce non-differentiability due to flux limiters, making exact linearization technically arduous and mathematically ill-defined [7, 8].

To overcome these barriers, we propose a non-intrusive, data-driven framework named the continuous local ensemble trained linear model (CLETLM), which eliminates the need for dedicated adjoint codes. The proposed method is inspired by the local ensemble tangent linear model (LETLM) [9] in meteorology. While LETLM estimates the time-evolution matrix from ensemble statistics, it inevitably suffers from approximation errors caused by telescopic operators during finite-time integration. In contrast, the present approach leverages the spatial locality inherent in hyperbolic systems, such as the compressible Navier–Stokes equations, and focuses on the residual response around the steady state rather than time evolution. This enables the highly accurate identification of the sparse Jacobian matrix of the spatial derivative terms, excluding the time-derivative term, in the continuous governing equations. A major advantage of this method is its ease of application, requiring only the addition of a residual output function to existing solvers and providing immediate access to the adjoint operator via a simple transposition of the explicitly identified matrix.

To validate the effectiveness of the proposed framework, this study conducts global stability and adjoint analyses of a two-dimensional compressible flow around a circular cylinder ($Re = 47 - 100$, $M_\infty = 0.1 - 0.3$). In this paper, we demonstrate that the proposed method correctly identifies the discrete Jacobian matrix and adjoint properties solely from primal forward simulation data on a baseline grid without requiring any adjoint code, by comparing the obtained unstable eigenvalues and spatial structures of the direct and adjoint modes with previous studies [10, 11].

2. Methodology

2.1 Numerical Method

The governing equations are the two-dimensional compressible Navier–Stokes equations. The working fluid is assumed to be an ideal gas, and the temperature dependence of the viscosity is considered using Sutherland's law [12]. A finite volume method is employed for spatial discretization. Inviscid fluxes are evaluated using the simple high-resolution upwind scheme (SHUS) [13], and viscous fluxes are computed using a second-order central difference scheme. For the interpolation of variables at cell interfaces, a third-order monotone upstream-centered scheme for conservation laws (MUSCL) approach without a flux limiter [14] is utilized. Time integration is performed using the computationally efficient alternating direction implicit-symmetric Gauss–Seidel (ADI-SGS) method [15, 16], with a time step of $\Delta t = 0.1$. To obtain the unstable steady base flow required for global stability analysis, the selective frequency damping (SFD) method [17] based on the fortified solution algorithm (FSA) [18] is adopted. The damping coefficient for the SFD method is set to $\chi = 0.1$, and the time integration is continued until the flow field reaches a sufficiently steady state.

2.2 Grid and Boundary Conditions

Figure 1 illustrates the coordinate system around the cylinder. A structured O-type grid is used, where ξ and η denote the azimuthal and radial directions, respectively. In this study, a grid with 258×121 points ($N_\xi \times N_\eta$) is employed. The minimum grid spacing on the cylinder surface is set to $0.005D$ relative to the cylinder diameter D. The grid spacing in the η direction expands geometrically with increasing distance from the cylinder.

Regarding boundary conditions, an adiabatic no-slip condition is imposed on the cylinder surface, setting the velocity to zero. The density ρ and pressure p on the surface are evaluated by zeroth-order extrapolation from the interior of the computational domain, accounting for the variation of the geometric Jacobian J in the generalized coordinate system. At the outer boundary in the η direction, characteristic boundary conditions based on Riemann invariants [19] are applied. Specifically, local inflow and outflow are determined by the normal velocity component, and the boundary values are constructed by combining characteristic variables propagating from the interior with the external freestream conditions. This approach suppresses non-physical wave reflections at the boundary while maintaining physical consistency. Periodic boundary conditions are applied in the ξ direction.

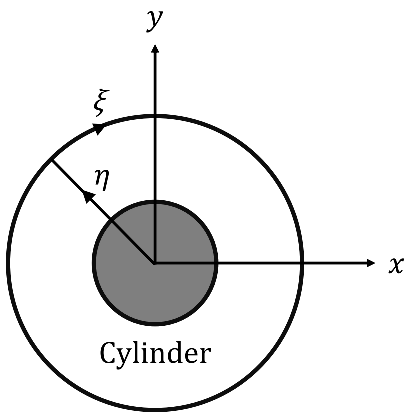

Figure 1: Coordinate system.

2.3 Computational Conditions

Table 1 summarizes the computational conditions tested in this study. The freestream Mach number M_∞ is set to 0.1, 0.2, and 0.3, and the Reynolds number Re ranges from 47 to 100. In the table, the checkmarks (✓) indicate conditions where unstable eigenvalues with positive growth rates were reported in the direct numerical simulation (DNS)-based global stability analysis by Canuto and Taira [10]. Conversely, the crosses (×) represent conditions where no unstable eigenvalues were reported in their study. The present validation focuses on the conditions where unstable eigenvalues exist.

Table 1: Computational conditions.

$M_\infty \setminus Re$	47	48	49	50	60	70	80	90	100
0.1	✓	✓	✓	✓	✓	✓	✓	✓	✓
0.2	×	✓	✓	✓	✓	✓	✓	✓	✓
0.3	×	×	✓	✓	✓	✓	✓	✓	✓

The working fluid is assumed to be air, with a specific heat ratio of $\gamma = 1.4$ and a Prandtl number of $Pr = 0.72$. The reference physical quantities for nondimensionalizing the governing equations are the cylinder diameter D, freestream density ρ_∞, and freestream speed of sound a_∞.

3. CLETLM

CLETLM is a data-driven framework designed to directly identify the Jacobian matrix of the discretized governing equations as a sparse matrix, using only forward simulation data. A major advantage of this approach is its non-intrusive nature; it can be applied to existing forward solvers with minimal modifications, requiring only the addition of a function to output residual responses.

3.1 Formulation

The spatially discretized two-dimensional compressible Navier–Stokes equations are written as:

$$\frac{\partial \mathbf{q}}{\partial t} = \mathbf{R}(\mathbf{q}), \tag{1}$$

where $\mathbf{q} = (\rho, \rho u, \rho v, e)^{\mathrm{T}}$ represents the state variable vector, and $\mathbf{R}(\mathbf{q})$ is the nonlinear residual vector. Applying Reynolds decomposition, the state variable $\mathbf{q}$ is separated into an unstable steady base flow $\bar{\mathbf{q}}$, which satisfies $\mathbf{R}(\bar{\mathbf{q}}) \approx 0$, and a small perturbation $\Delta\mathbf{q}$:

$$\mathbf{q} = \bar{\mathbf{q}} + \Delta\mathbf{q}. \tag{2}$$

Substituting Eq. (2) into Eq. (1) and performing a Taylor expansion of the nonlinear residual vector $\mathbf{R}(\bar{\mathbf{q}} + \Delta\mathbf{q})$ around the base flow $\bar{\mathbf{q}}$ yields:

$$\mathbf{R}(\bar{\mathbf{q}} + \Delta\mathbf{q}) = \mathbf{R}(\bar{\mathbf{q}}) + \left.\frac{\partial\mathbf{R}}{\partial\mathbf{q}}\right|_{\bar{\mathbf{q}}} \Delta\mathbf{q} + O(\|\Delta\mathbf{q}\|^2). \tag{3}$$

Here, the residual response $\Delta\mathbf{s}$ induced by the injected perturbation $\Delta\mathbf{q}$ is defined as:

$$\Delta\mathbf{s} = \mathbf{R}(\bar{\mathbf{q}} + \Delta\mathbf{q}) - \mathbf{R}(\bar{\mathbf{q}}). \tag{4}$$

By neglecting the higher-order terms of $O(\|\Delta\mathbf{q}\|^2)$ in Eq. (3), a linear relationship between $\Delta\mathbf{s}$ and $\Delta\mathbf{q}$ is established through the Jacobian matrix $\mathbf{A}$:

$$\Delta\mathbf{s} \approx \mathbf{A}\Delta\mathbf{q}, \tag{5}$$

$$\mathbf{A} = \left.\frac{\partial\mathbf{R}}{\partial\mathbf{q}}\right|_{\bar{\mathbf{q}}}. \tag{6}$$

In the CLETLM framework, the matrix $\mathbf{A}$ is identified by injecting random perturbations $\Delta\mathbf{q}$ into the solver, collecting a large number of corresponding residual responses $\Delta\mathbf{s}$, and utilizing these $(\Delta\mathbf{q}, \Delta\mathbf{s})$ pairs as ensemble data.

3.2 Exploitation of Spatial Locality

Hyperbolic systems, including the compressible Navier–Stokes equations, possess inherent spatial locality. Consequently, the residual response Δs_i at a specific grid point i depends exclusively on the local perturbations $\Delta\mathbf{q}_{i,\mathrm{local}}$ within its adjacent numerical stencil. This property allows us to assume that the matrix $\mathbf{A}$ is extremely sparse. By exploiting this locality, CLETLM decomposes the identification of $\mathbf{A}$ into independent, small-scale least-squares problems for each grid point, thereby dramatically reducing the computational burden.

Let N_v be the number of state variables per grid point, and let the index k $(= 1, \ldots, N_v)$ distinguish these components. Assuming the reference stencil contains N_s points based on the spatial discretization scheme, the number of unknown coefficients (non-zero elements) in each row of $\mathbf{A}$ is $N_\mathrm{nz} = N_\mathrm{v} \times N_\mathrm{s}$. We define a local row vector $\mathbf{a}_{i,k} \in \mathbb{R}^{1\times N_\mathrm{nz}}$ that extracts these N_nz unknown coefficients for component k at grid point i. Given K $(\geq N_\mathrm{nz})$ sets of ensemble data, the local residual response vector $\Delta\mathbf{S}_{i,k} \in \mathbb{R}^{K\times 1}$ is defined as:

$$\Delta\mathbf{S}_{i,k} = [\Delta s_{i,k}^{(1)}, \Delta s_{i,k}^{(2)}, \ldots, \Delta s_{i,k}^{(K)}]^\mathrm{T}. \tag{7}$$

Similarly, the local perturbation matrix $\Delta\mathbf{Q}_{i,k} \in \mathbb{R}^{K\times N_\mathrm{nz}}$, consisting of the local perturbations within the stencil, is defined as:

$$\Delta\mathbf{Q}_{i,k} = [\Delta\mathbf{q}_{i,\mathrm{local}}^{(1)}, \Delta\mathbf{q}_{i,\mathrm{local}}^{(2)}, \ldots, \Delta\mathbf{q}_{i,\mathrm{local}}^{(K)}]^\mathrm{T}. \tag{8}$$

The linear response relationship for $\mathbf{a}_{i,k}$ can then be expressed as $\Delta\mathbf{S}_{i,k} = \Delta\mathbf{Q}_{i,k}\mathbf{a}_{i,k}^\mathrm{T}$. The optimal solution $\mathbf{a}_{i,k}$ that minimizes the sum of squared errors is obtained by solving the following least-squares problem:

$$\mathbf{a}_{i,k} = \arg\min_{\mathbf{x}} \|\Delta\mathbf{S}_{i,k} - \mathbf{x}\Delta\mathbf{Q}_{i,k}\|_2^2. \tag{9}$$

This procedure is repeatedly applied to every grid point i and component k. The complete Jacobian matrix $\mathbf{A}$ is then constructed by assembling the obtained $\mathbf{a}_{i,k}$ into their corresponding rows.

For the two-dimensional compressible Navier–Stokes equations used in this study, the number of state variables is $N_{\mathrm{v}} = 4$. Figure 2 illustrates the specific numerical stencil adopted. The nine axial points (blue), including the target cell (red), represent the evaluation range for the inviscid fluxes by the SHUS and third-order MUSCL schemes. The four diagonal points (light blue) correspond to the evaluation range for the viscous fluxes by the second-order central difference scheme. Thus, the total number of stencil points is $N_{\mathrm{s}} = 13$, resulting in $N_{\mathrm{nz}} = N_{\mathrm{v}} \times N_{\mathrm{s}} = 52$ non-zero elements per row.

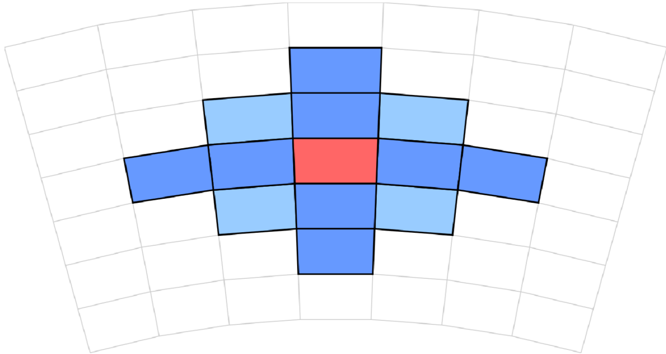

Figure 2: Schematic of the 13-point stencil.

3.3 Global Stability Analysis

The asymptotic stability of the base flow $\bar{\mathbf{q}}$ is evaluated by examining the unstable eigenvalues of the matrix $\mathbf{A}$. The eigenvalue problem governing the linear response of perturbations around $\bar{\mathbf{q}}$ is given by:

$$\mathbf{A}\mathbf{v} = \lambda\mathbf{v}, \tag{10}$$

where λ is a complex eigenvalue and $\mathbf{v}$ is the direct mode. If an eigenvalue with a positive real part exists, the base flow is considered unstable.

Conversely, the adjoint mode $\mathbf{w}$ is defined as the left eigenvector of the matrix $\mathbf{A}$:

$$\mathbf{w}^{\mathrm{H}}\mathbf{A} = \lambda\mathbf{w}^{\mathrm{H}}. \tag{11}$$

Taking the Hermitian conjugate of both sides yields the following eigenvalue problem:

$$\mathbf{A}^{\mathrm{T}}\mathbf{w} = \lambda^*\mathbf{w}, \tag{12}$$

where λ^* represents the complex conjugate of λ. Since $\mathbf{A}$ is a real matrix, its Hermitian conjugate is equivalent to its transpose ($\mathbf{A}^{\mathrm{H}} = \mathbf{A}^{\mathrm{T}}$). A significant benefit of the proposed method is that adjoint modes can be extracted simply by transposing the identified matrix $\mathbf{A}$, eliminating the need for dedicated adjoint code development.

Since the size of the identified matrix $\mathbf{A}$ reaches $O(10^5 \times 10^5)$, it is practically impossible to compute all its eigenvalues directly. Therefore, the shift-and-invert Arnoldi (SIA) method [20] is employed to efficiently extract eigenvalues near an arbitrary complex shift point σ_{shift}. Equations (10) and (12) are transformed as follows:

$$(\mathbf{A} - \sigma_{\mathrm{shift}}\mathbf{I})^{-1}\mathbf{v} = \frac{1}{\lambda - \sigma_{\mathrm{shift}}}\mathbf{v}, \tag{13}$$

$$(\mathbf{A}^T - \sigma^*_{\mathrm{shift}}\mathbf{I})^{-1}\mathbf{w} = \frac{1}{\lambda^* - \sigma^*_{\mathrm{shift}}}\mathbf{w}. \tag{14}$$

Through this mapping, eigenvalues λ closer to σ_{shift} in the complex plane are mapped to eigenvalues with larger absolute values, enabling efficient extraction by the Arnoldi method.

The extracted eigenvalues λ are initially nondimensionalized based on the speed of sound a_∞. To compare these results with the previous DNS-based study [10], which used the freestream velocity U_∞ for normalization, the growth rate σ_r and the frequency σ_i are rescaled using the freestream Mach number M_∞:

$$\sigma_\mathrm{r} = \frac{\mathrm{Re}(\lambda)}{M_\infty}, \quad \sigma_\mathrm{i} = \frac{\mathrm{Im}(\lambda)}{2\pi M_\infty}. \tag{15}$$

4. Results

In this section, the proposed CLETLM framework is applied to the global linear stability analysis of a two-dimensional compressible flow around a circular cylinder. The investigation is performed at a freestream Mach number of $M_\infty = 0.1$, spanning a Reynolds number range from $Re = 47$ to 100. The quantitative accuracy of the identified unstable eigenvalues is verified first, followed by a qualitative assessment of the spatial structures of both the direct and adjoint modes.

4.1 Validation of Eigenvalues

The unstable eigenvalues identified by the framework are quantitatively compared with the reference DNS results of Canuto and Taira [10]. Figure 3 displays the variations in the growth rate σ_r and frequency σ_i with respect to the Reynolds number.

As illustrated in Fig. 3, the CLETLM successfully captures the qualitative physical trends for both the growth rate σ_r and the frequency σ_i with respect to the Reynolds number. However, the identified values are quantitatively underestimated compared to the reference data. This discrepancy is considered to stem from the influence of the spatial resolution employed in this study. The spatial discretization inherently introduces numerical errors, causing the discrete system to deviate from the true continuous governing equations. It is expected that refining the grid would lead the results to asymptotically approach the continuous system. Therefore, these results indicate that the CLETLM accurately extracts the exact dynamic characteristics of the given discrete system itself, fully encompassing its numerical properties.

4.2 Validation of Direct and Adjoint Modes

The spatial structures of the identified direct and adjoint modes at $Re = 47$ and $M_\infty = 0.1$ are compared with the incompressible results of Marquet et al. [11]. Under this low Mach number condition, density fluctuations are assumed to be negligible, and the identified momentum components $(\rho u, \rho v)$ are directly compared with the reference velocity components (u, v).

Figure 4 presents the spatial distributions of the leading direct and adjoint modes. The direct mode (Figs. 4 (a) and (b)) exhibits a characteristic wave packet that propagates and amplifies toward the downstream wake region. This spatial pattern is in good agreement with the reference study, maintaining a physically appropriate structure.

Furthermore, the adjoint mode (Figs. 4 (c) and (d)) clearly visualizes the upstream receptivity of the flow. The spatial oscillations localized upstream of the cylinder are successfully captured. Although minor discrepancies are observed in the peak amplitudes near the cylinder surface, the global wave structures governing the system's instability are accurately reproduced. These results demonstrate that the CLETLM can successfully identify the adjoint properties of a fluid system purely from forward simulation data, circumventing the complex derivation of adjoint equations.

5. Conclusion

This paper presented the continuous local ensemble trained linear model (CLETLM), a non-intrusive, data-driven framework enabling global linear stability and adjoint analyses without requiring adjoint codes. By leveraging the inherent spatial locality of numerical stencils in hyperbolic systems, such as

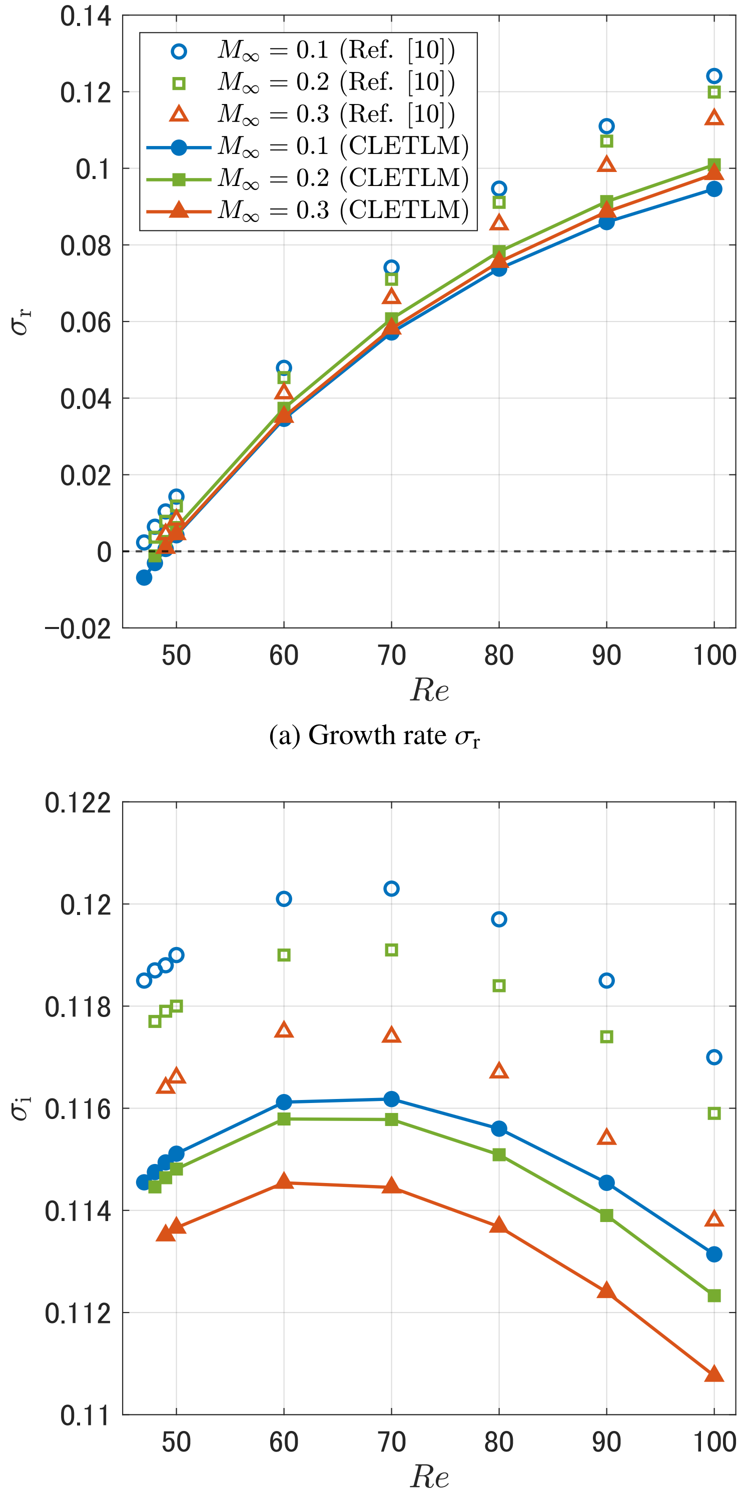

(a) Growth rate σ_r

(b) Frequency σ_i

Figure 3: Comparison of identified eigenvalues λ with the previous study [10].

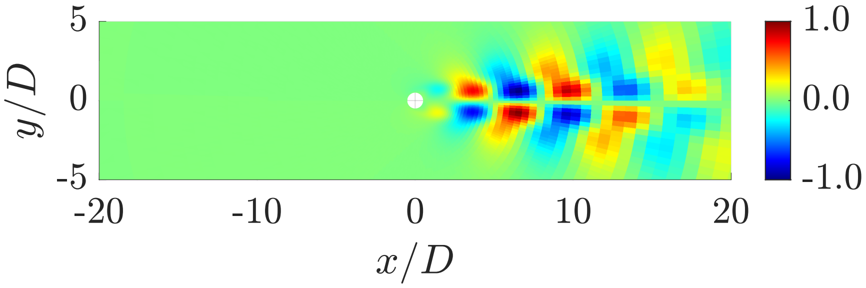

(a) Direct mode ρu

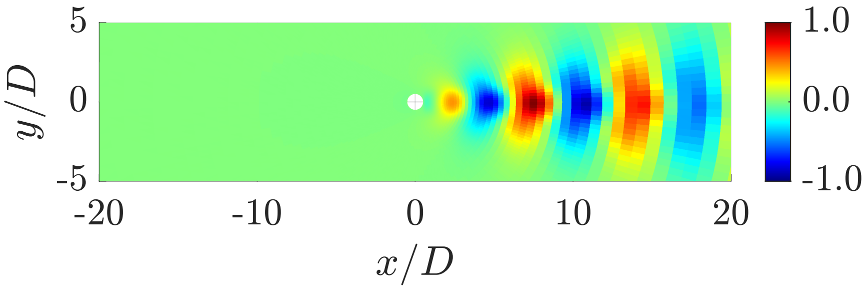

(b) Direct mode ρv

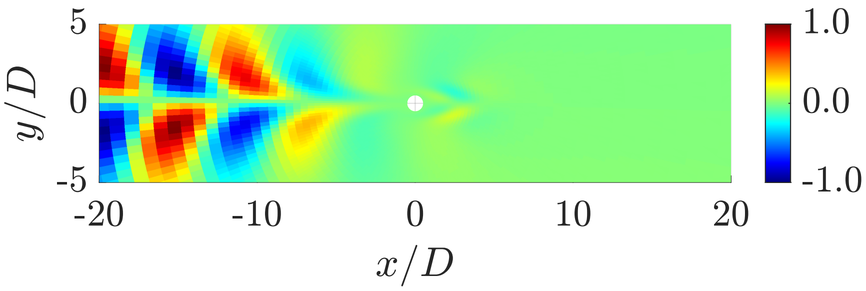

(c) Adjoint mode $\rho u^\dagger$

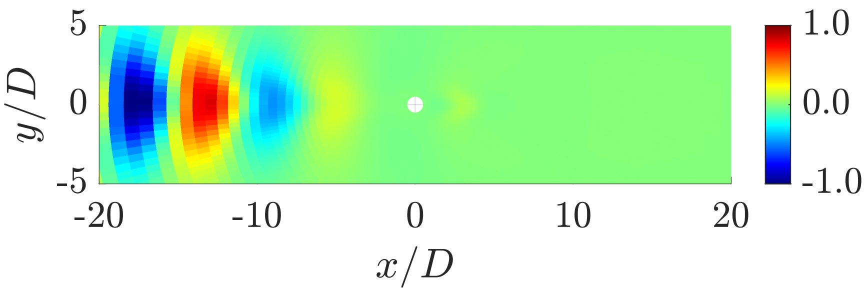

(d) Adjoint mode $\rho v^\dagger$

Figure 4: Spatial distributions of the identified (a, b) direct and (c, d) adjoint modes ($Re = 47$, $M_\infty = 0.1$).

the compressible Navier–Stokes equations, the proposed approach explicitly constructs a sparse Jacobian matrix directly from the residual responses of a standard forward solver.

The effectiveness of the framework was validated through its application to a two-dimensional compressible flow past a circular cylinder at $M_\infty = 0.1$ and $Re = 47$–100. The results demonstrated that the CLETLM successfully captured the qualitative physical trends of the unstable eigenvalues. Furthermore, the quantitative discrepancies arising from the spatial resolution employed in this study suggested that the method faithfully extracts the exact linear dynamics of the underlying discrete system, properly reflecting its numerical properties. Additionally, the spatial distributions of the leading direct and adjoint modes were successfully reproduced, confirming the method's ability to capture both the downstream propagating wave packet and the upstream receptivity.

These findings strongly support the effectiveness of the CLETLM in identifying adjoint properties purely from forward simulation data, allowing researchers to bypass the arduous implementation of adjoint codes. Future work will include applying the present framework to higher Mach number flows. Furthermore, we plan to extend the framework to unstructured grids to enable stability analyses around complex geometries, and to consider the application of the identified discrete Jacobian matrix to flow control, thereby expanding the practical utility of the framework.

References

[1] Antony Jameson. Aerodynamic design via control theory. *Journal of scientific computing*, 3(3):233–260, 1988.

[2] François-Xavier Le Dimet and Olivier Talagrand. Variational algorithms for analysis and assimilation of meteorological observations: theoretical aspects. *Tellus A: Dynamic Meteorology and Oceanography*, 38(2):97–110, 1986.

[3] Beverley J McKeon and Ati S Sharma. A critical-layer framework for turbulent pipe flow. *Journal of Fluid Mechanics*, 658:336–382, 2010.

[4] Clarence W Rowley. Model reduction for fluids, using balanced proper orthogonal decomposition. *International Journal of Bifurcation and Chaos*, 15(03):997–1013, 2005.

[5] Michael B Giles and Niles A Pierce. An introduction to the adjoint approach to design. *Flow, turbulence and combustion*, 65(3):393–415, 2000.

[6] Dana A Knoll and David E Keyes. Jacobian-free newton–krylov methods: a survey of approaches and applications. *Journal of Computational Physics*, 193(2):357–397, 2004.

[7] Mike Giles and Stefan Ulbrich. Convergence of linearized and adjoint approximations for discontinuous solutions of conservation laws. part 1: Linearized approximations and linearized output functionals. *SIAM Journal on numerical analysis*, 48(3):882–904, 2010.

[8] Mike Giles and Stefan Ulbrich. Convergence of linearized and adjoint approximations for discontinuous solutions of conservation laws. part 2: Adjoint approximations and extensions. *SIAM Journal on Numerical Analysis*, 48(3):905–921, 2010.

[9] Craig H Bishop, Sergey Frolov, Douglas R Allen, David D Kuhl, and Karl Hoppel. The local ensemble tangent linear model: An enabler for coupled model 4d-var. *Quarterly Journal of the Royal Meteorological Society*, 143(703):1009–1020, 2017.

[10] Daniel Canuto and Kunihiko Taira. Two-dimensional compressible viscous flow around a circular cylinder. *Journal of fluid mechanics*, 785:349–371, 2015.

[11] Olivier Marquet, Denis Sipp, and Laurent Jacquin. Sensitivity analysis and passive control of cylinder flow. *Journal of Fluid Mechanics*, 615:221–252, 2008.

[12] William Sutherland. Lii. the viscosity of gases and molecular force. *The London, Edinburgh, and Dublin Philosophical Magazine and Journal of Science*, 36(223):507–531, 1893.

[13] Eiji Shima and T Jounouchi. Role of cfd in aeronautical engineering (no. 14). *AUSM Type Upwind Schemes, NAL SP-34*, 1997.

[14] W Kyle Anderson, James L Thomas, and Bram Van Leer. Comparison of finite volume flux vector

splittings for the euler equations. *AIAA journal*, 24(9):1453–1460, 1986.

[15] Shigeru Obayashi, Kozo Fujii, and S. Gavali. Navier-Stokes simulation of wind-tunnel flow using LU-ADI factorization algorithm. Technical Report NASA TM-100042, NASA, feb 1988.

[16] Hiroyuki Nishida and Taku Nonomura. ADI-SGS scheme on ideal magnetohydrodynamics. *Journal of Computational Physics*, 228:3182–3188, 2009.

[17] Espen Åkervik, Luca Brandt, Dan S Henningson, Jérôme Hœpffner, Olaf Marxen, and Philipp Schlatter. Steady solutions of the navier-stokes equations by selective frequency damping. *Physics of fluids*, 18(6), 2006.

[18] Kozo Fujii. Unified zonal method based on the fortified solution algorithm. *Journal of Computational Physics*, 118(1):92–108, 1995.

[19] Antony Jameson and Timothy Baker. Solution of the euler equations for complex configurations. In *6th computational fluid dynamics conference danvers*, page 1929, 1983.

[20] Yousef Saad. *Numerical methods for large eigenvalue problems: revised edition*. SIAM, 2011.